

Constraining the critical groundwater conditions for initiation of large, irrigation-induced landslides, Sigwas River Valley, Peru



Abstract In the last three decades, a series of large landslides have occurred in the Sigwas River Valley, Peru, and their causes have been attributed to irrigation input affecting the local groundwater conditions. While the causal relationship of the irrigation water to these landslides is widely accepted, the actual groundwater conditions necessary to initiate these landslides have not been previously quantified. In this paper, we present finite element modeling work to estimate the critical groundwater conditions required to initiate failure for the Zarzal and Pachaqui Chico Landslides, given back-calculated strength parameters, topography, and remote estimates of the likely range of possible groundwater scenarios. Modeling results indicate that elevated groundwater tables are required for landslide initiation and that these elevated groundwater tables are more likely due to perched zones forming from irrigation water input, rather than from elevation of the original deeper water table. In addition, the moisture content outside the saturated zone appears to be a less significant factor in landslide initiation than the position and configuration of the saturated zones. These results compare favorably to groundwater data acquired since the initiation of these landslides. Understanding of the groundwater conditions at initiation is important for designing mitigation to help prevent future landslides, and several mitigation options are briefly discussed.

Keywords Peru · Sigwas River Valley · Landslide initiation · Irrigation-induced landslides · Large landslides · Finite element method

Introduction

Groundwater has a fundamental influence on the stability of slopes. High water tables increase driving forces by adding weight to the slope and reduce resisting forces by increasing pore pressures in the slide mass. Downslope, ponded water can provide a buttress against sliding, but groundwater present along sliding surfaces can reduce effective stress and therefore decrease the shear strength of geomaterials. Seepage forces from moving groundwater can also contribute to reduced resisting forces, depending on the rate and flow direction of groundwater. Landslide initiation can result from disturbances to natural groundwater systems due to natural causes, including precipitation events and flooding, and due to anthropogenic causes such as reservoir filling and irrigation. Rapid addition of water to the slide mass (i.e., from irrigation, flooding, or rainfall) or rapid drawdown of a buttressing reservoir can trigger landslide movement.

Irrigation-induced landslides are a global phenomenon (Garcia-Chavesich et al. 2021). Examples of these landslides have been

studied in California (Knott 2008), British Columbia (Clague and Evans 2003), Mexico (Villaseñor-Reyes et al. 2018), China (e.g., Zhang et al. 2009; Li and Jin 2012; Xu et al. 2012; Peng et al. 2018), Palu, Indonesia (Bradley et al. 2019; Watkinson and Hall 2019), Tajikistan (domej et al. 2019), Pakistan (Ali et al. 2017), and southern Peru (Lacroix et al., 2020). Some of these landslides have been attributed entirely to irrigation triggering (Li and Jin 2012), while others have been attributed to multiple effects (e.g., irrigation cause and seismic trigger [Bradley et al. 2019; Watkinson and Hall 2019], or irrigation cause and high rainfall trigger [Knott 2008; Villaseñor-Reyes et al. 2018]). Irrigation-induced landslides have occurred in a variety of geologic settings, such as loess (Peng et al. 2018), volcanogenic sediments (Villaseñor-Reyes 2018), alluvium (Bradley et al. 2019), and lacustrine sediments (Clague and Evans 2003). Depending on the local geology, slope, groundwater conditions, and the presence of other causal or triggering factors, irrigation-induced landslides can have a variety of failure modes, including lateral spreads (Bradley et al. 2019), debris flows/long runout landslides (Bradley et al. 2019), flowslides (Peng et al. 2018), and deep-seated gravitational slope deformations (Villaseñor-Reyes et al. 2018).

Three features of irrigation-induced landslides appear in multiple case studies. First, irrigation water typically only affects slopes that are downhill from the irrigated area. Irrigated zones associated with landslides can be a simple hillslope with an irrigation channel uphill of the fields (slopes can be steep: domej et al. 2019, or shallow: Bradley et al. 2019), or a plateau or mesa above a river valley (e.g., Clague and Evans 2003; Li and Jin 2012; Lacroix et al. 2020). Second, periods of relatively high landslide velocity or landslide initiation often correspond to periods of high irrigation outputs (e.g., the dry season or periods of below-average rainfall) (Clague and Evans 2003; Knott 2008; Villaseñor-Reyes et al. 2018). By contrast, rainfall-initiated landslides tend to occur or accelerate during the wet season. Third, irrigation-induced landslides appear more commonly with high discharge rates of irrigation water, such as flood irrigation (Clague and Evans 2003) or leaking/damaged irrigation canals and storage pools (Zhang et al. 2009; Ali et al. 2017). In one study in British Columbia, after these high discharge methods had been exchanged for more efficient, sprinkler irrigation, landslide initiation decreased significantly, and no more large landslides were observed (Clague and Evans 2003).

Large volume irrigation can result in perched groundwater systems in slopes. For the purposes of this study, a perched water table is considered to be a saturated zone that is distinct from a deeper saturated zone and is perched atop a relatively low permeability feature, such as a lithologic boundary (e.g., clay, shale, igneous

sill) (Carter et al. 2011) or structural discontinuities (e.g., jointing or faulting) (Wyllie and Mah 2004). In complex geology, multiple perched water tables can exist. For the perched zone to be considered distinct from the deeper groundwater system, there must be an unsaturated (or dry) zone between them. Perched groundwater can develop when water infiltrates down to a low-permeability layer, including water sourced irrigation, or from rainfall (Van Asch et al. 1996; Greco et al. 2018), irrigation (Xu et al. 2012; Zhang and Liu 2010), or melting snow and ice (Patton et al. 2019).

Intuitively, a perched water table is likely to decrease the Factor of Safety (FS) of a slope. However, the effect of a perched water table combined with a deeper saturated zone may not be the same as a shallower, single groundwater table because of the lower total volume of saturated material in the slope. For large landslides, large volumes of groundwater can be required to generate sufficient pore pressures across a larger shear surface to destabilize the whole mass (Van Asch et al. 1999).

Relatively few studies have focused on the effects of perched zones on slope stability, though several studies have included references to perched groundwater in discussions of landslide triggering processes (e.g., Xu et al. 2012; Zhang and Liu 2010). Van Asch et al. (1996) found that a perched water table supplied lower zones with water, controlling the stability of the overall slope for a large landslide in varved clays. Their infiltration experiments and simulations indicated landslide velocity was primarily affected by changes in pore water pressure in fissures within the clay units, rather than by seepage along layers. Based on their infiltration calculations, they concluded that drainage of the top layer of the slope would help to reduce landslide movement (Van Asch et al. 1996).

Landslide modeling allows the user to back-calculate values or ranges of values for unknown parameters (shear strength, failure plane geometry, groundwater, etc.) based on the parameters that are better constrained (Wyllie and Mah 2004). In most cases, models are prepared using as much data as possible to constrain conditions, and the remaining parameters are adjusted until the model reaches the desired FS. Use of landslide modeling allows the user to back-calculate the “critical” conditions for the slope: that is, the conditions within the slope at the time of failure. This study focuses on estimating the critical groundwater conditions at the instant of landslide initiation, when the FS is lowered just below 1, thereby initiating slope failure, regardless of the rate of subsequent landslide movement. Previous studies have used both numerical modeling methods (Preisig 2020; Zhou et al. 2020) and limit equilibrium methods (Beyabanaki et al. 2016; Chiliza and Hingston 2018; Salinas-Josso et al. 2020) to evaluate critical groundwater conditions.

Irrigation-induced landslides are a key geologic hazard near important irrigation projects in the Arequipa region of southern Peru. While it is widely accepted that many of the recent landslides in this region were caused by excess irrigation water, several aspects of the relationship between groundwater and landslide initiation remain poorly understood. This paper describes finite element method (FEM) modeling efforts to better understand and quantify important aspects of the critical groundwater conditions for two landslides in the Sigüas River Valley, Southern Peru including whether a perched zone is present in these slopes, the depth of the water table at the time of landslide initiation and the probable moisture content of geomaterials outside the saturated zones. We begin by describing the study area, the landslides examined

in this paper, and the limited data available on local groundwater conditions. We then present the modeling approach, methods, and results. Finally, we conclude by discussing the implications of the modeling results for local groundwater conditions and for landslide mitigation in the region.

Case study background

Overview of the study area and history of landsliding

The Sigüas River, near Arequipa in southern Peru, provides water to irrigated agricultural land on the pampas (broad coastal plateaus) to the northwest (NW) of the river valley and to a small area of agricultural land within the valley, adjacent to the river. The Majes-Sigüas irrigation project has diverted water from the Sigüas River to irrigate otherwise extremely arid land and increase the agricultural capacity of the region since the 1980s. Beginning in the early 2000s, several large landslides with various movement modes, volumes, and rates of movement have occurred in the Sigüas River Valley (Hermanns et al. 2012; Lacroix et al. 2020). Some of these landslides move slowly and gradually (m/year – tens of m/year), such as the Zarzal Landslide (also called the “Sigüas Landslide” as in Lacroix et al. (2019, 2020)). Other landslides likely proceeded as rapid rock avalanches, with velocities on the order of m/s, such as the Pachaqui Grande and Pachaqui Chico Landslides. These landslides have produced a variety of hazards to local communities, including loss of crop-land, erosion of the valley flanks, damming of the Sigüas River and flooding, and threats to local infrastructure. This paper explores critical groundwater conditions for the Zarzal Landslide and the Pachaqui Chico Landslide (Fig. 1).

The stratigraphy at the Zarzal and Pachaqui Chico Landslides includes two primary units (Instituto Geológico Minero y Metalúrgico (INGEMMET) 2008; Graber et al. 2020). The lowest relevant layer is the Paleogene-Neogene Moquegua Fm. which is composed primarily of sandstones and some conglomerates, with some shale and tuff units. A thick (~10 m) thick, probably-unwelded tuff is frequently found at the top of the Moquegua in this area. For the purposes of modeling, this particular tuff is included in the model stratigraphy as its own unit, since it is expected to influence the overall strength of the slope. The Moquegua is overlain by the Neogene Millo Fm., which consists primarily of conglomerates and gravels of variable cementation.

Most published works on landslides in the Sigüas River Valley have focused their attention on the Zarzal Landslide (Fig. 1A, B), because it presents a direct threat to the nearby Pan-American Highway and a nearby industrial milk processing plant. Published studies of the Zarzal Landslide include Araujo Huamán et al. (2016), Araujo (2017), Araujo et al. (2017), Meza Arestegui and Chacon Arcaya (2017), Lacroix et al. (2019), and Graber et al. (2020). The Zarzal Landslide is a large, retrogressive landslide that initiated in 2005 (Araujo et al. 2017; Lacroix et al. 2019). Recent studies estimate the landslide volume to be ~40 M m³ (Araujo 2017; Lacroix et al. 2019). The headscarp is estimated to be retreating at rates of 4.4–71 m/year (Araujo 2017). Because the landslide has undergone multiple retrogressions since initiation, there are likely multiple slip surfaces within the slide mass, and new slip surfaces are likely formed as each major retrogression detaches a new block from the headscarp (Araujo Huamán et al. 2016; Lacroix et al. 2019).

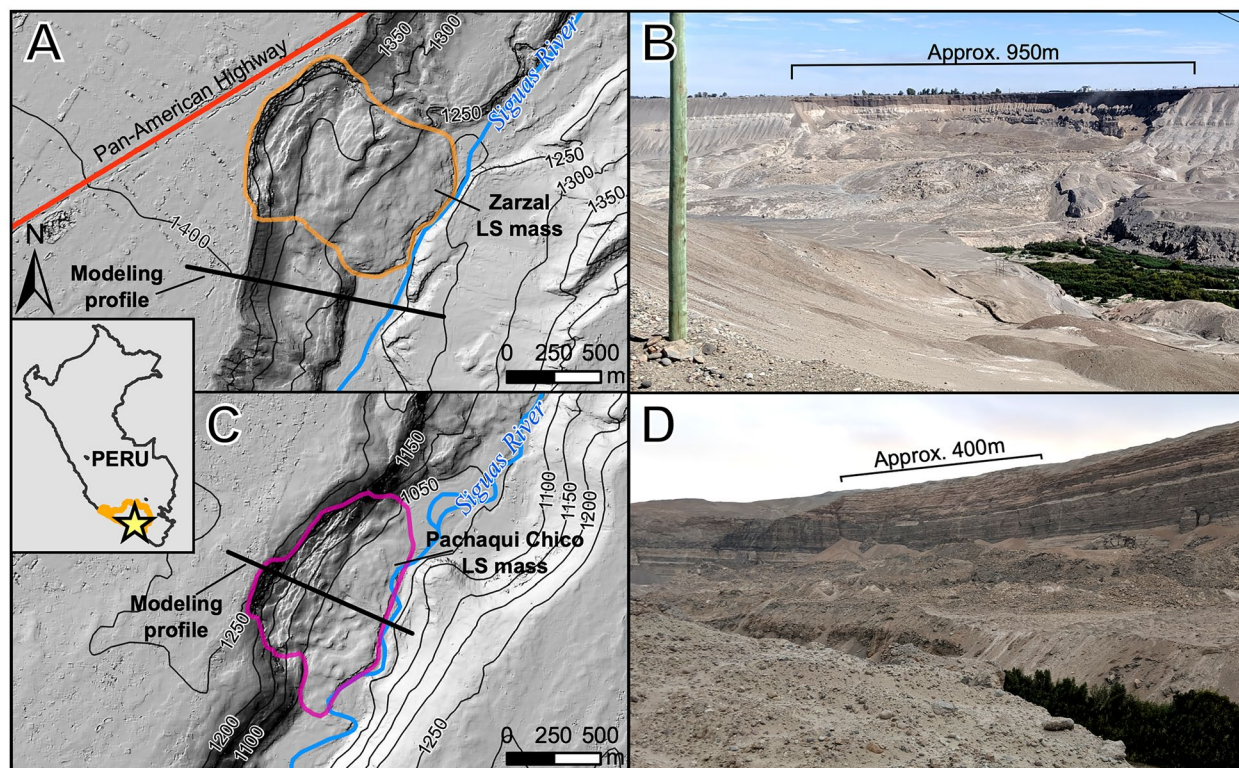


Fig. 1 **A** Hillshade of Zarzal Landslide (lat/long: -16.369769° , -72.155715°) as of 29 May 2015. A pre-failure digital elevation model (DEM) was not available for Zarzal, so the modeling profile was extracted from the 4 Aug 2014 DEM using an adjacent similar slope (see the “[Model set-up, strength parameters, and groundwater variables](#)” section). Note proximity of the headscarp to the Pan-American Hwy. **B** Photo of Zarzal Landslide, 17 July 2019, looking W from near the Pan-American Hwy. on the east (E) side of the Sigwas Valley. Note the terraced topography to the right and left of the landslide. **C** Hill-

shade of Pachaqui Chico Landslide (lat/long: -16.444618° , -72.188829°) as of 29 May 2015. The modeling profile was extracted from a pre-failure DEM representing the topography as of 4 Aug 2014. **D** Photo of Pachaqui Chico Landslide 17 July 2019, looking SW from near the E bank of the Sigwas River. Note the steep scarp and that disturbed landslide material is present on both sides of the river (foreground). 2 m basemap hillshade in **A** and **C** credit (Lacroix et al. 2019). Contour interval for **A** and **C** is 50 m. Photos in **B** and **D** taken by K. Radach, summer 2019.

The Pachaqui Chico Landslide (Fig. 1C, D), in contrast to the slow, retrogressive failure of the Zarzal Landslide, represents a fast moving, rock avalanche style failure that occurred in essentially a single event. Review of Google Earth and Planet.com satellite images brackets the Pachaqui Chico Landslide between 16 May and 28 Aug 2014. The Pachaqui Chico slide does not appear in a DEM based on 4 Aug 2014 images collected by an AIRBUS satellite, further constraining the main failure timing to 4–28 Aug 2014. While some antecedent movement of the slope prior to the main failure is suggested by Lacroix et al. (2020), satellite images indicate that the main failure occurred over a timescale much shorter than that of Zarzal. The difference in failure mode of these landslides results in distinctly different post-failure topography (compare the blocky, undulating mass in Fig. 2A with the steep scarp and flatter landslide mass in Fig. 2B).

Beyond the Sigwas Valley, large landslides are a regional problem in southern Peru. Landslide hazards have been identified by inventories prepared for the Peruvian government in the Chili, Sigwas, and Vitor river valleys (Fidel Smoll et al. 1997; Zavala et al. 2012), the Colca and Camaná river valleys (Kosaka Masuno et al. 2001) and more generally in the Arequipa region (Luque Poma

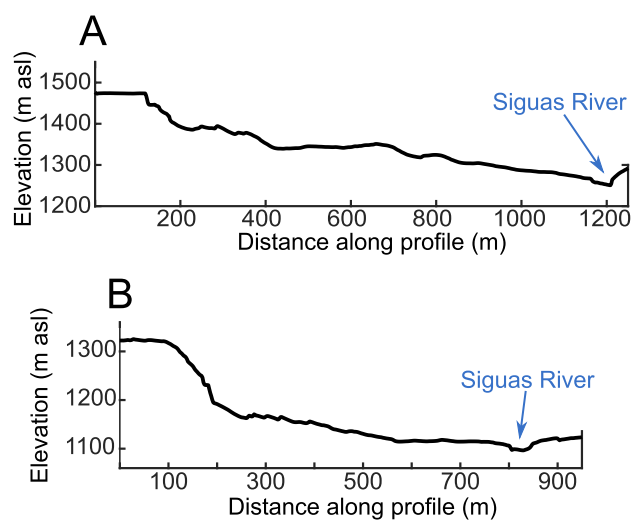


Fig. 2 Post-failure profiles extracted from a 2-m DEM (Lacroix et al. 2019) along the centerlines of **A** Zarzal and **B** Pachaqui Chico Landslides

and Rosado Seminario 2014). Landslides attributed to irrigation are present in the Sigvas Valley and in the Vítor Valley to the south (S) (Hermanns et al. 2012; Araujo Huamán and Miranda Cruz 2016; Lacroix et al. 2020), as well as in the Colca Valley to the north (N) (Gómez Avalos 2017; Roberti et al. 2018). In the Sigvas and Vítor valleys, both prehistoric and irrigation-induced landslides are present (Fig. 3), with the greater number of known failures having occurred since the beginning of irrigation.

The Vítor River Valley, to the southeast (SE) of the Sigvas River Valley, has experienced a similar history of recent, large landslides (Fig. 3). While both valleys have experienced prehistoric landslides on both sides of the valley (Hermanns et al. 2012; Araujo 2017), all the landslides that have occurred since the onset of irrigation (in the 1980s for Sigvas; 1950s for the N end of Vítor, 1970s for the S end of Vítor) appear on the irrigation sides of the valley (Fig. 3). As a result, the recent landslides in this area appear to be directly related to excess water input from irrigation (Hermanns et al. 2012; Araujo Huamán and Miranda Cruz 2016; Araujo et al. 2017; Meza Arestegui and Chacon Arcaya 2017; Lacroix et al. 2020).

The hazard impact of landslides in the Majes-Siguas area has been variable. Some slides occur at the valley flanks away from the irrigated pampas and only override cropland within the river valley itself. Others override valley cropland while simultaneously eroding from the pampas and destroying irrigated cropland. Larger landslides in the Sigvas Valley have dammed the Sigvas river in multiple locations, causing temporary flooding of upstream areas. The Zarzal Landslide is probably the most plainly hazardous landslide in this area because it is simultaneously overriding valley cropland (and previously dammed the river) while eroding the upper surface of the pampa, retrogressing towards the Pan-American Highway and the industrial milk processing plant just across the highway. LiDAR monitoring of the headscarp suggests that the headscarp may reach the highway and the milk processing facility within the next few years (Araujo et al. 2017).

This paper studies the Zarzal and Pachaqui Chico landslides because they represent two end-members for irrigation-induced landsliding in the Sigvas Valley. The Sigvas and Vitor Valleys contain other examples both of fast-moving and slow-moving landslides, and the hazard implications of different movement velocities

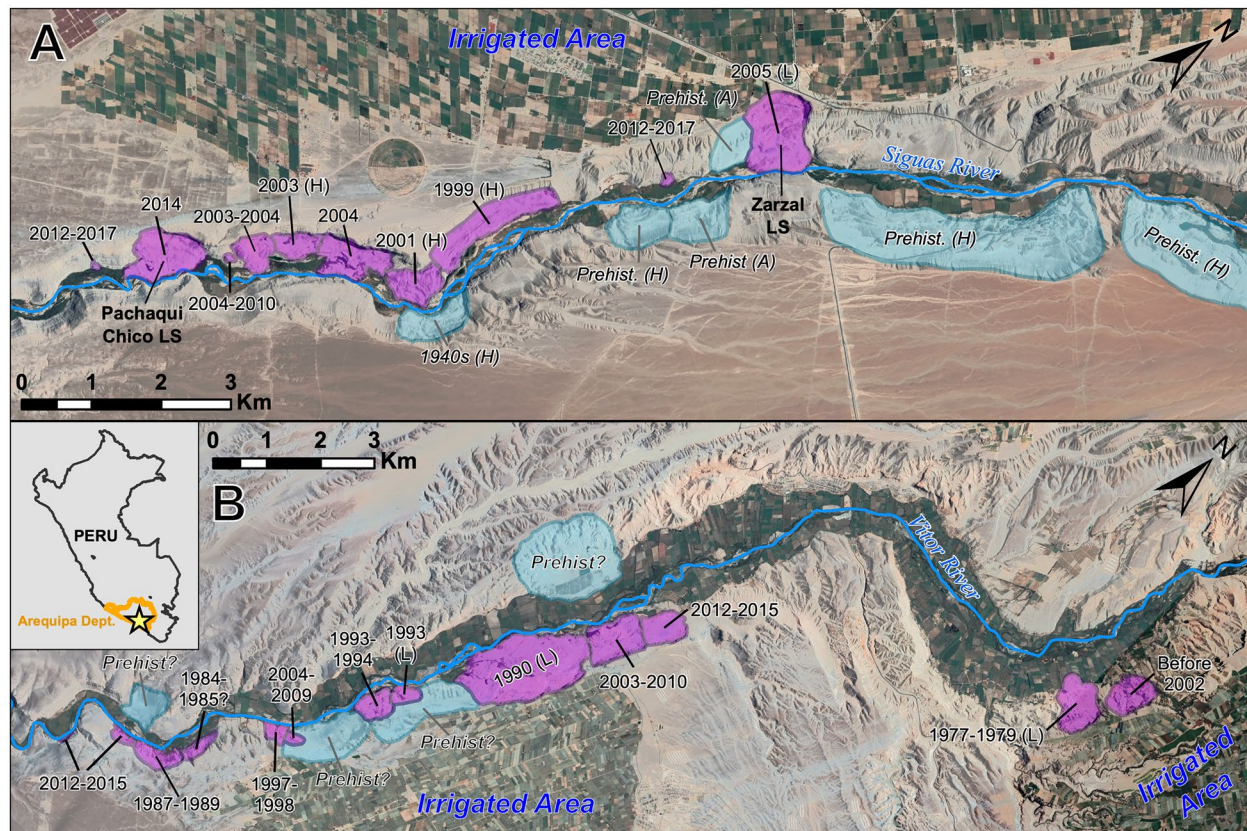


Fig. 3 Spatial relationship of landslides and irrigated land for **A** Sigvas River Valley and **B** Vitor River Valley. While both valleys have several large, prehistoric landslides (blue polygons), the majority of the landslides in these valleys initiated since the start of irrigation (purple polygons). These recent landslides are invariably located on the side of the valley adjacent to the irrigated land. This figure incorporates originally mapped landslides with landslides previously mapped by Hermanns et al. (2012), Araujo (2017), and Lacroix et al.

(2020). Prehistoric landslides marked with a “?” are uncertain. Where possible, landslides have been labeled with estimated year of initiation and a letter to indicate the source of the date: H (Hermanns et al. 2012), A (Araujo 2017), or L (Lacroix et al. 2020). Dates with no letter were estimated for this paper using Google Earth imagery. Satellite imagery credit: Copyright 2021 Google, Image Copyright 2021 CNES/Airbus, Image Copyright 2021 Maxar Technologies

can potentially be different. So, the effect of groundwater and the expected triggering conditions need to be understood in both cases in order to inform mitigation efforts.

Available groundwater information

The Sigüas River flows at the base of the Sigüas Valley, near the toes of several slide masses. Because the area around the Zarzal Landslide is extremely arid (annual precipitation is typically < 1 cm/year, Lacroix et al. [2019]), the Sigüas River likely represents a losing stream (contributing water to the local groundwater system, rather than gaining from the groundwater system).

Geophysical surveys taken in 2006 (Instituto Nacional de Recursos Naturales [INRENA], 2006) were interpreted to indicate a ~100–200 m thick, low-resistivity zone present at depth within the Moquegua Fm. INRENA (2006) concluded that this zone represented a thick, generally continuous clay layer with the top of the unit at depths of ~70–150 m throughout the area (see blue contours in Fig. 4A) and that this clay layer forms a perched aquifer (indicated by moderate resistivity in their surveys) and directs excess irrigation water to flow out of the NW wall of the Sigüas Valley. At Zarzal, the depth to this layer is reported to be ~80 m (Fig. 4A), while at Pachacqui Chico, the depth is reported to be ~135–150 m. These depths fall around the midpoint of each slope. However, the presence of a 100–200 m thick clay layer does not fit well with local geologic mapping of the Moquegua Fm., which is dominated by sandstones with some conglomerate and clay layers (Guizado Jol 1968). Considering this description of the geology, the variability in the depth of the clay layer of INRENA (2006) may imply that

there is no single thick, continuous clay layer: rather that there may be discontinuous clay layers in the region and the net effect of these is to cause perched aquifers.

Springs are present in the NW Sigüas Valley wall in ~20 locations (Fig. 4A) and are believed to represent excess water from irrigation (Araujo et al. 2017). Similar springs have been observed on the irrigation side (SE) of the Vitor Valley (Araujo Huamán and Miranda Cruz 2016). These springs have appeared in different places along the valley flanks at least since 2004. In some cases, water has also been observed flowing out of the landslide masses themselves (Araujo et al. 2017). The locations and elevations of springs in the valley flank were mapped using Google Earth imagery from five dates between 2004 and 2019 and elevation information from a 12-m resolution DEM of the study area (Fig. 4A). When plotted, the spring elevations versus the depth to the clay layer (INRENA, 2006) at the same location fall approximately along a 1:1 line (Fig. 4B) (correlation coefficient, 0.92; $R^2 = 0.85$). The median absolute difference between the estimated clay layer elevations and the spring elevations from the 2014 DEM is just 23 m (std. dev. 18 m). Because of the correlation between the estimated clay layer depths and the associated spring elevations, these two datasets data imply that there is some subsurface feature that is controlling at least part of the irrigation water and causing it to form a perched zone, such that excess water flows out of the valley around the midpoint of the slope.

A sizeable pond (~3000m² in area, volume is unknown) exists at the industrial facility just NW of the Zarzal Landslide (Fig. 4A). From review of Google Earth images, this facility was established around 2002, just 3 years before the Zarzal Landslide was initiated

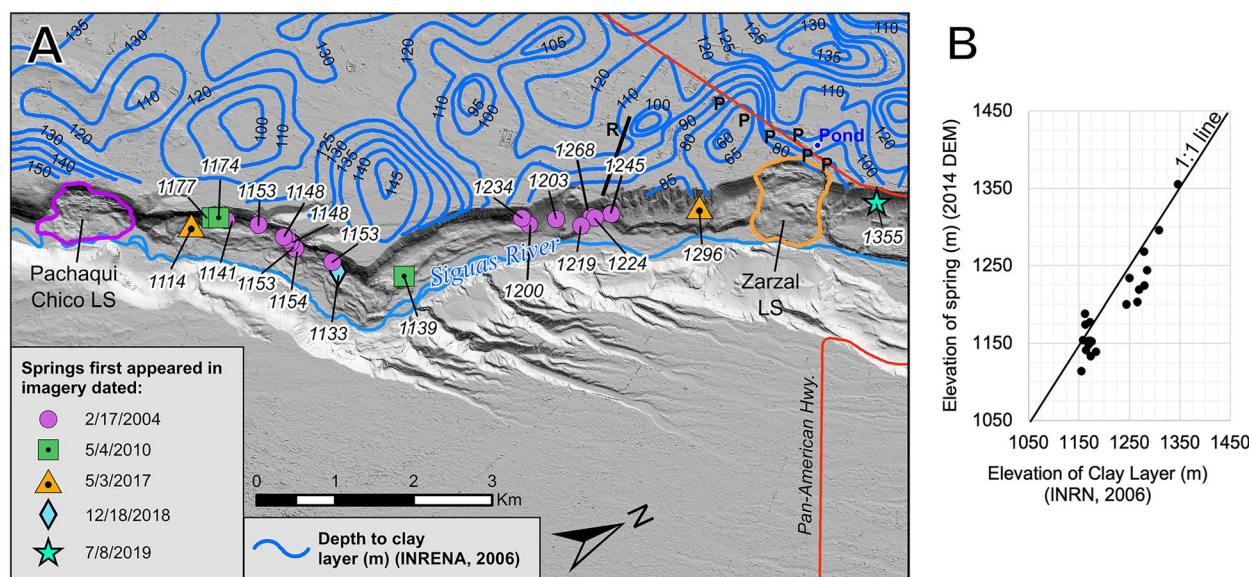


Fig. 4 A Summary of available groundwater data. Blue contours represent the estimated depth to the clay layer from INRENA (2006). Colored markers give locations and elevations of springs. The black "P's" mark the locations of piezometers measured Jan 2019 (Gonzales Zenteno E, personal communication 2021) and the "R" and black line mark the location of the 2019 resistivity profile (Flamme et al. 2020) (see the "Comparison with other estimations of local ground-

water conditions" section). 2 m DEM hillshade represents topography as of 29 May 2015 (Lacroix et al. 2019). **B** Scatter plot of spring elevations taken from the 12-m DEM versus clay layer elevations taken from INRENA (2006) data for the slope above each spring. The good correlation between the two (correlation coefficient 0.92, $R^2 = 0.85$) suggests that the springs are related to the local elevation of the clay layer

in 2005 (Araujo et al. 2017; Lacroix et al. 2019). If the pond liner leaks, the lost water may flow towards the Zarzal Landslide, contributing additional water to any local groundwater systems that are present.

In 2019, two additional data sources became available. Water level measurements were collected at 6 piezometers near the Zarzal headscarp (Fig. 4A), finding that the water depth varied from 108 m at the northernmost piezometer, to 81 m at the southern end of the line of piezometers (Gonzales Zenteno E, personal communication, 2021). In addition, a resistivity profile was taken about 2 km S of the Zarzal Landslide (marked with an “R” in Fig. 4A) (Flamme et al. 2020). This profile indicated that a saturated zone exists from ~100 to 190 m below the area it was taken. These data were excluded from model development because they were collected several years after landslide initiation, so they do not necessarily reflect the critical groundwater conditions. However, they can be used as a point of comparison for modeling results (see the “Comparison with other estimations of local groundwater conditions” section).

Methods

Overview

To estimate the critical groundwater conditions for the Zarzal and Pachaqui Chico Landslides, we begin with calibrated pre-failure models and strength parameters (Graber et al. 2020) and then test a variety of possible groundwater conditions to find which scenarios result in $FS < 1$ for each slope. The scenarios that produce FS values just below 1 are taken to be the minimum conditions required to initiate a landslide, given the model inputs. Though both slopes have similar geology and stratigraphy, their pre-failure slope morphologies (Fig. 5) and failure modes (see the “Overview of the study area and history of landsliding” section) are distinct,

necessitating testing of both profiles to evaluate any differences in critical groundwater conditions.

Model groundwater scenarios

At least two possible groundwater scenarios may be interpreted based on the information from the “Available groundwater information” section and can be applied to both the Zarzal and Pachaqui Chico pre-failure slopes. The scenarios chosen for this study are represented schematically in Fig. 5. First, the additional input of water from irrigation may have simply elevated the natural groundwater table on the NW side of the valley (Fig. 5A, C), while groundwater levels remain low on the opposite side of the valley (assuming the natural groundwater profile near the Sigwas River is that of a losing stream). Because the irrigation input is limited to the NW side of the valley (from the Majes-Siguas irrigation project), the increase in water table elevation would only be present within the NW flank of the valley. In this case, the observed flow of groundwater out of the slope at various locations along the NW slope may perhaps be explained by the presence of a more permeable zone that causes water to exit the slope near the middle elevation.

Alternately, the presence of a low-permeability layer (or layers) at the approximate midpoint elevation of the slope, as suggested by INRENA (2006), combined with the springs appearing at corresponding elevations may indicate that there is a perched groundwater zone, separate from a deeper groundwater system associated with the Sigwas River (see Fig. 5B, D). It should be noted that this perched zone could also be caused by a relatively high permeability layer, instead of water perched on top of a low-permeability layer. In either case, the primary cause of the perched zone would be permeability contrasts between units in the slope. If a perched zone is

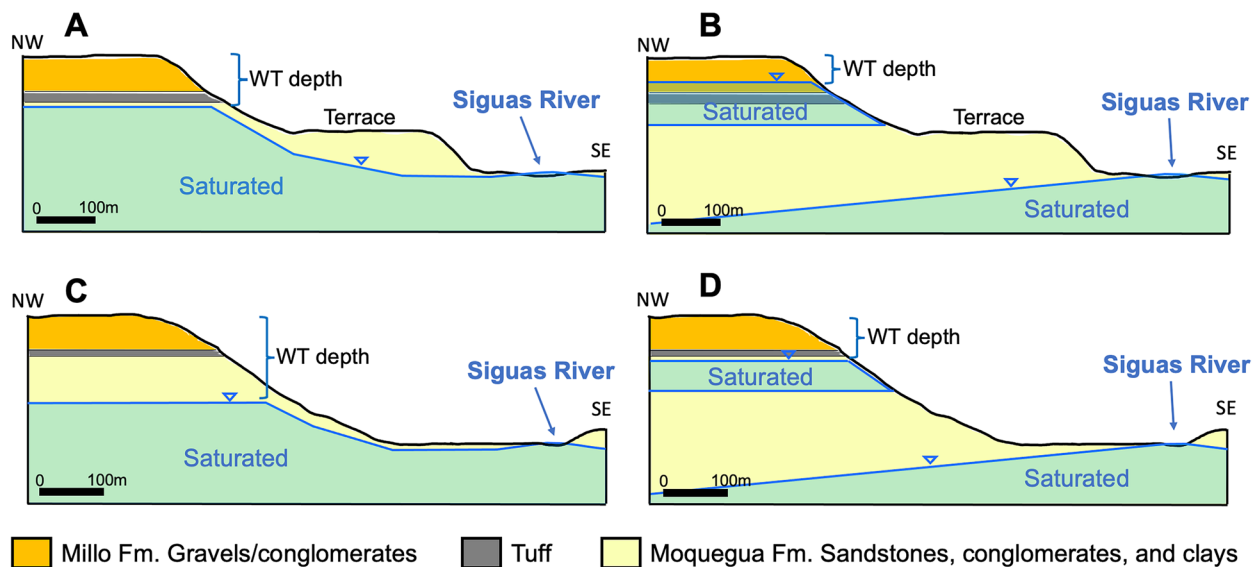


Fig. 5 Schematic representations of end-member groundwater scenarios. **A** Single saturated zone with elevated water table on irrigation side of valley with Zarzal pre-slide topography. **B** Two separate saturated zones with Zarzal pre-slide topography. **C** Single saturated zone with elevated water table with Pachaqui Chico pre-slide topog-

raphy. **D** Two separate saturated zones with Pachaqui Chico pre-slide topography. The water table depth used as a model variable is marked with “WT depth”. Saturated zones are indicated. Approximate scales are given; no vertical exaggeration

present, the lower groundwater system associated with the Sigüas River likely takes the shape of a losing stream profile, while the perched zone sits at some elevation above. Assuming that the drainage of water from the springs is controlled by a low-permeability layer at depths corresponding to those reported by INRENA (2006), the base of the perched zones probably falls near the midpoint of the slope. The unsaturated zone between the two saturated zones could be relatively dry or relatively close to saturation.

The evidence is currently inconclusive as to which of these scenarios best represents reality. Both of these scenarios would cause an increase in the amount of water present in the slope, though the positions and thicknesses of the saturated zones are likely to differ between these two scenarios. Of course, the real scenario may be the result of a combination of an elevated in situ groundwater table and creation of a perched zone. We chose to test a range of water table elevations for both scenarios to evaluate the relative likelihood of landslide initiation under different scenarios.

Additionally, the input of irrigation water into the slopes above these landslides may result in partial saturation of materials above the water table. Increased partial saturation increases the unit weights of the relevant geomaterials and therefore increases the driving forces, potentially affecting the stability of the slope (Ray et al. 2010). While data is unavailable on the in situ moisture content of the materials above the water table, we tested a separate group of models to evaluate whether elevated, but unsaturated, moisture content is likely to contribute to landslide initiation.

This research assumes that the primary groundwater changes resulting from irrigation are “bottom to top” increases in the elevation of the water table which would then increase positive pore water pressure, rather than considering the effects of other hydrological landslide triggers, such as soil suction or seepage force (Brönnimann 2011). In addition, it is assumed that pore pressures in the aquifer(s) result only from the depth of water in the saturated zone, rather than from any confined water pressure.

Model set-up, strength parameters, and groundwater variables

Models were constructed and run using Rocscience RS2 software (Version 11.003). RS2 is a finite element software for modeling 2-dimensional geologic scenarios (typically slopes and tunnels) to compute relevant geomechanical information such as stress and strain. Using the shear strength reduction (SSR) method, RS2 is also used for slope stability analysis. The SSR method computes a Critical Strength Reduction Factor (Critical SRF) by iteratively reducing the input strength parameters and computing FEM models until acceptable tolerances are reached (Hammah et al. 2005). The Critical SRF is mathematically equivalent to the FS, and it represents the amount by which the input strength parameters must be reduced to cause model instability. If the Critical SRF is > 1 , the model slope is stable, as with the FS. If the Critical SRF is < 1 , the model slope is unstable. Hammah et al. (2005), Graber et al. (2020), and Rocscience (2021) give additional background on RS2 theory and application.

To construct FEM models for the Zarzal and Pachaqui Chico Landslides, we used topography extracted along straight line profiles (locations in Fig. 1(A, C)) taken from a 12-m DEM based on the AIRBUS global DEM (imagery date: 4 Aug 2014) purchased from L3Harris Geospatial. The data for this DEM were captured prior to the Pachaqui Chico failure, so the Pachaqui Chico profile reflects

the pre-slide topography. For the Zarzal Landslide, a pre-failure DEM was not available in sufficient resolution for FEM modeling. Based on review of satellite images of Zarzal taken prior to the main failure (Fig. 6), we observed that the adjacent slope has very similar physiography to the pre-failure slope of Zarzal: both slopes include a terraced area in the middle with a relatively small slope below the terrace and a larger slope above. Given the similarity between the two slopes, we chose to extract topography from the adjacent slope to serve as the model topography for the Zarzal FEM models.

Model strength parameters (Table 1) were assigned according to previous work on the Zarzal Landslide that used Geological Strength Index ratings, Schmidt Hammer readings, and literature values in combination with FEM modeling to back-calculate a set of strength parameters for the materials of interest (Graber et al. 2020). The Generalized Hoek–Brown strength criterion was used for all models. A porosity value of 20% was used for all model materials. This value is a reasonable literature value for the lithologies that dominate the slope of the Sigüas River Valley, including sandstones and conglomerates (Manger, 1963) and unwelded tuffs (Smyth and Sharp 2006). The SSR method was used to compute the Critical SRF for each model, and these values were used as the primary point of comparison between models. For simplicity, we refer to the critical SRF values as FS values, but both terms are noted on relevant plots in the “Results” section.

Two analyses were performed given two general groundwater scenarios at two slopes resulting in a total of eight groups of models. Table 2 summarizes the model cases and variables for both analyses. The first analysis was designed to test the height of groundwater in the upper portion of the slope that would be required to initiate

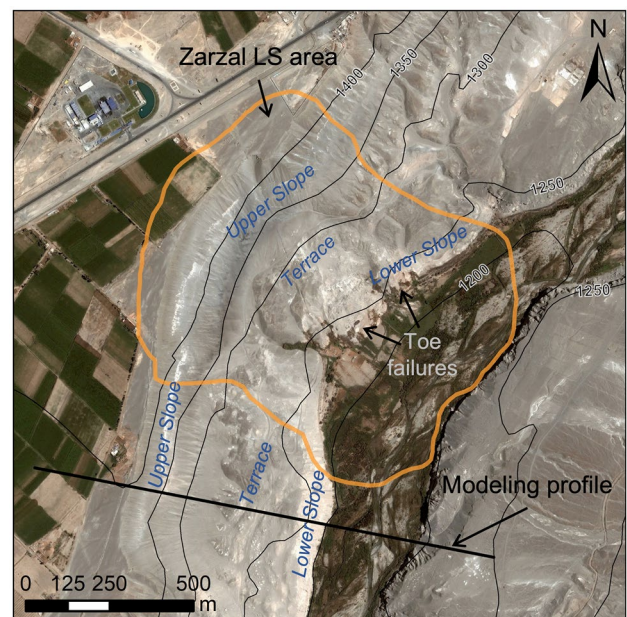


Fig. 6 17 Feb 2004 satellite image of Zarzal Landslide and adjacent slope prior to the primary failure of Zarzal. Note the similarities between the Zarzal slope and the adjacent slope where the modeling profile was taken, and the small failures from the lower slope of Zarzal. Contours give elevation in m. Image credit: Google Earth, Copyright 2021 Maxar Technologies.

Table 1 Summary of material strength values used for model units (values from Graber et al. 2020)

Parameter	Millo Fm	Tuff	Moquegua Fm
UCS (MPa)	1.1	3.5	3.15
Hoek–Brown intact rock constant, m_i	21	13	17
Intact elastic modulus (MPa)	16,500	5500	37,000
Unit Weight (dry, MN/m ³)	0.022	0.016	0.027
Poisson's ratio	0.25	0.2	0.25
–	<i>Peak/Residual</i>	<i>Peak/Residual</i>	<i>Peak/Residual</i>
Geological Strength Index (GSI)	30/12	40/15	40/10
m_b	1.724/0.906	1.525/0.625	1.994/0.683
s	0.0004189/0.0000567	0.0012726/0.0000791	0.0012726/0.0000454
a	0.5223/0.5747	0.5114/0.5611	0.5114/0.5854
Calculated rockmass modulus (MPa)	1342.8/537.4	878.1/200.5	5907.1/1128.6

landsliding. A series of different model cases with different groundwater elevations in the upper slope, with all other parameters constant, was prepared for both slopes and both groundwater scenarios. Because the groundwater data for this area are limited and coarse in resolution (see the “Available groundwater information” section), we chose to represent groundwater using the relatively simple static water table method in RS2. In this method, saturated conditions are applied below the piezometric line(s), while materials above the water table are assumed to be dry. The model then computes the saturated unit weight of materials below the piezometric line based on the input dry unit weight and porosity and applies the appropriate values in the SSR calculation. Model material boundaries were used to control where saturated conditions were applied for the perched zones. Groundwater depths in the upper portion of

each slope were varied in 10 m increments measured from the top of the slope (Fig. 7). The models with the deepest water tables that resulted in an FS value less than 1 were taken to indicate the minimum water table elevation required for landslide initiation. We refer to this depth as the “landslide initiation depth”.

The second analysis was designed to test the possibility that non-zero moisture content in the unsaturated zone(s) could contribute to landslide initiation at these slopes by increasing the unit weight of unsaturated materials, and therefore the driving forces. For this group of models, the base cases for both groundwater scenarios and both slopes were taken to be the models from the landslide initiation depth analysis with the highest water table heights that still resulted in FS values of 1 (1.01 for Pachaqui Chico with one saturated zone). The unit weights of all dry materials in the model were then increased

Table 2 Summary of analyses, model cases, and variables

Analysis		Zarzal Landslide		Pachaqui Chico Landslide	
		One saturated zone	Two saturated zones	One saturated zone	Two saturated zones
Landslide initiation depth	Range of water table depths below the top of the slope tested (10 m increments)	10–130	20–130	130–290	30–140
	Total models	13	12	17	12
Moisture content of unsaturated zones	% moisture content for unsaturated zone(s)	5, 10, 15, 17.5	5, 10, 15, 17.5	5, 10, 15, 17.5	5, 10, 15, 17.5
	WT depth for the moist unit weight models	20 m	40 m	230 m	100 m
	FS value for moist unit weight base case	1	1	1.01	1
	Total models	4	4	4	4
Overall Total Model Cases		17	16	21	16

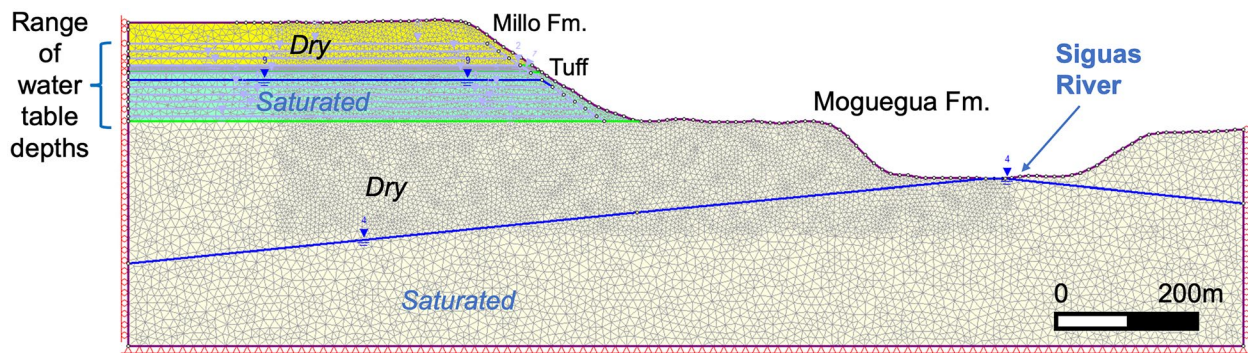


Fig. 7 Example RS2 finite element model used for analysis. Note the range of water table elevations in the upper slope, boundary constraints (pins along the base and rollers along the sides), and overall mesh density. Water table depth is measured from the top of the slope

according to moisture content increases (values of 5%, 10%, 15%, and 17.5% were modeled) to evaluate whether higher moisture content in the unsaturated zone(s) would be likely to change these models from a condition of meta-stability ($FS = 1$) to instability ($FS < 1$).

Results

Figure 8 presents the results of the groundwater initiation depth analysis. Some scatter is present in the FS values returned by the FEM models for both analyses in this paper. This scatter is probably due in large part to the inherent precision capabilities of the RS2 implementation of the SSR Method. The precision is limited because of the accumulated effect of small random errors in RS2 solution process. Because of this error in the FS values, we report a range of values as the estimate of the water table depth required for landslide

initiation. This range is given as the shallowest water table depth for FS just less than 1 to the deepest water table depth for $FS = 1$ (or $FS = 1.01$ for the Pachaqui Chico Models with a single saturated zone, Fig. 8B), because $FS = 1$ represents a metastable condition.

As a result, the landslide initiation groundwater depths indicated by the modeling analysis are 10–40 m for the Zarzal Landslide with a single saturated zone, 30–60 m for the Zarzal Landslide model with two separate saturated zones, 220–240 m for the Pachaqui Chico Landslide with a single saturated zone, and 90–100 m for the Pachaqui Chico Landslide with two saturated zones. The two landslides respond differently to the two groundwater scenarios: for Zarzal, the single saturated zone landslide initiation depth is shallower, while for Pachaqui Chico, the two saturated zone landslide initiation depth is shallower (see the

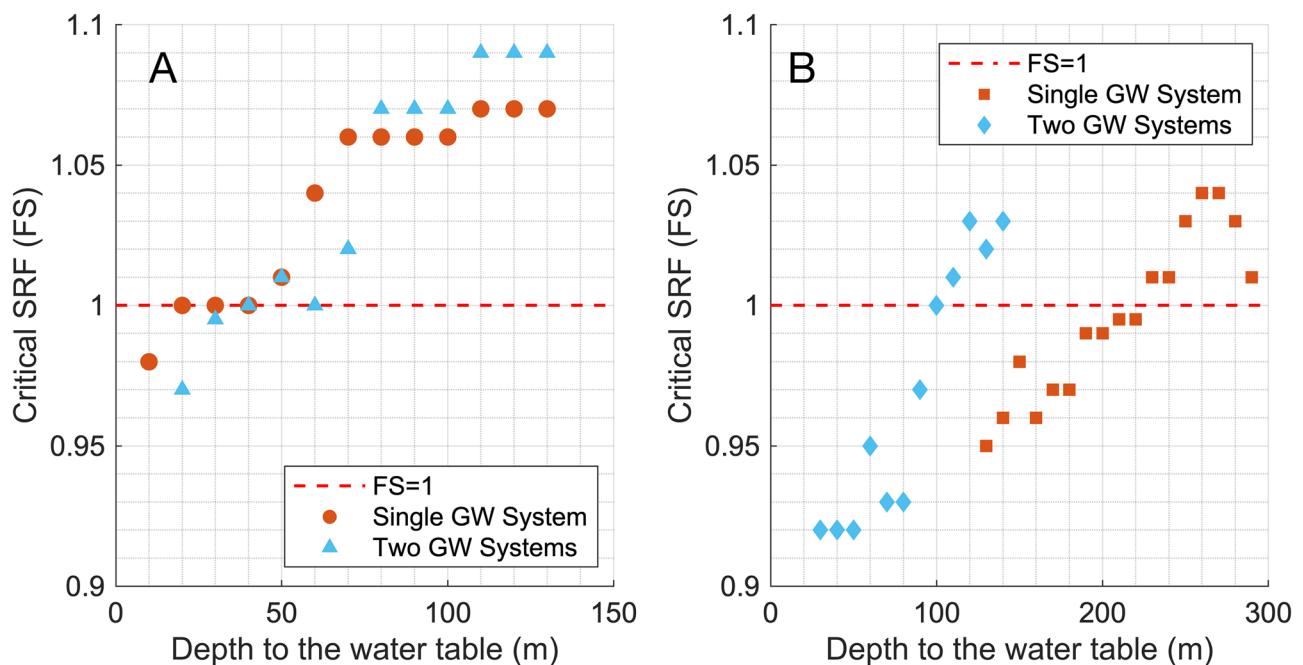


Fig. 8 Plots of the depth to the water table in the upper portion of the slope vs critical SRF for **A** the Zarzal Landslide slope profile and **B** the Pachaqui Chico slope profile. The water table depth for the

first model with $FS < 1$ is taken to be the minimum water table depth required to initiate model instability

“Implications of modeling results for critical groundwater conditions” section for a discussion of this difference).

Figure 9 presents the results of the moist unit weight analysis. The results show the expected overall decrease in FS with increasing moisture content in the unsaturated zone(s) for both slopes and both groundwater scenarios, but there is also some scatter in the results. In some cases, an increase in the moisture content in the saturated zone results in a higher FS value than the previous model with a lower unsaturated moisture content (Fig. 9). Please refer to the “Implications of modeling results for critical groundwater conditions” section for a discussion of this variability and the implications of these results.

Figure 10 illustrates the range of failure surfaces indicated by the models for both slopes and both groundwater scenarios at the landslide initiation depth. At both landslides, the failure surfaces are non-circular. For the Zarzal Landslide, the failure surfaces are similar for both groundwater scenarios. However, for the Pachaqui Chico Landslide, the failure surface is notably shallower in the perched groundwater scenario than when there is only one saturated zone in the model.

Discussion

Implications of modeling results for critical groundwater conditions

Given the input material property values calibrated in a previous study (Graber et al. 2020), the FS values for these models range from ~0.9–1.1. The highest FS value in any model was 1.14 for a

set of conditions that included only the presumed losing stream groundwater profile associated with the Sigwas River. These relatively low FS values seem to be reasonable given the history of pre-historic and modern landslides in this valley (Hermanns et al. 2012; Araujo 2017) and in other neighboring river valleys (e.g., Lacroix et al. 2020).

The Zarzal Landslide models indicate that an elevated groundwater table in the upper slope is required to initiate a landslide, regardless of whether one or two saturated zones is present. This slope may be relatively stable against landslide initiation with deeper groundwater tables due to the buttressing effect of the lower terrace at that slope (Fig. 5A, B). While the estimated groundwater depth required for landslide initiation is similar for both scenarios, the perched zone scenario seems much more likely due to the observation that raising the in situ groundwater table about 200 m from what would likely have been the original position (lower water table in Fig. 5B) seems unrealistic for the level of irrigation input (median daily irrigation use at the Majes-Siguas project is about 15 m³/s from 2009 to 2017 for an irrigated area of ~170km², with a slight overall decline in that period, Wei X, personal communication [2021]) at Majes and the total time of irrigation (since the mid-1980s).

For the Pachaqui Chico Landslide, the depth of the model failure surface is affected by the model groundwater scenario. A perched zone near the middle of the slope produces a model failure surface that exits near the lower ¼ of the slope (Fig. 10D), while a single saturated zone results in a deeper failure plane (Fig. 10C). For this landslide, it is possible that the failure was

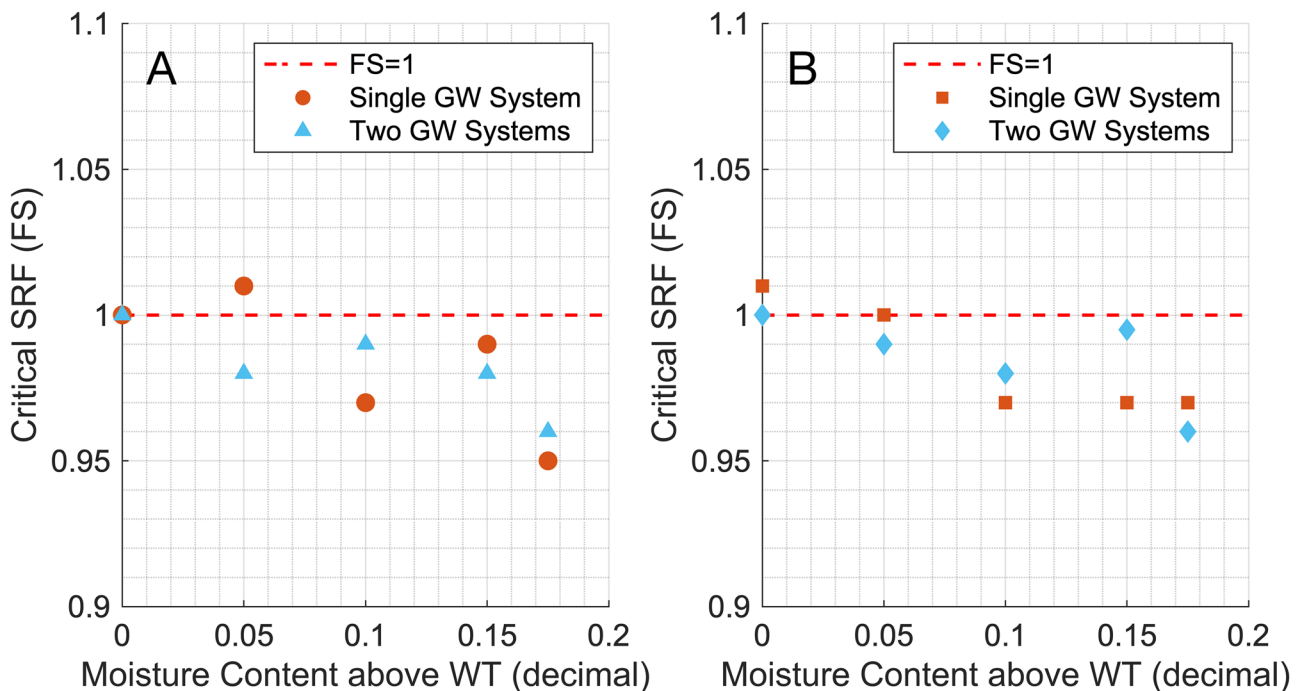


Fig. 9 Scatter plots of modeling results for model cases with increasing moist unit weight above the water table for **A** Zarzal Landslide and **B** Pachaqui Chico Landslide. In each case, a slight decrease is observed in FS with increasing moisture content. How-

ever, there is also some scatter in each group of results, with some cases showing an apparent increase in FS resulting in a further increase in moisture content

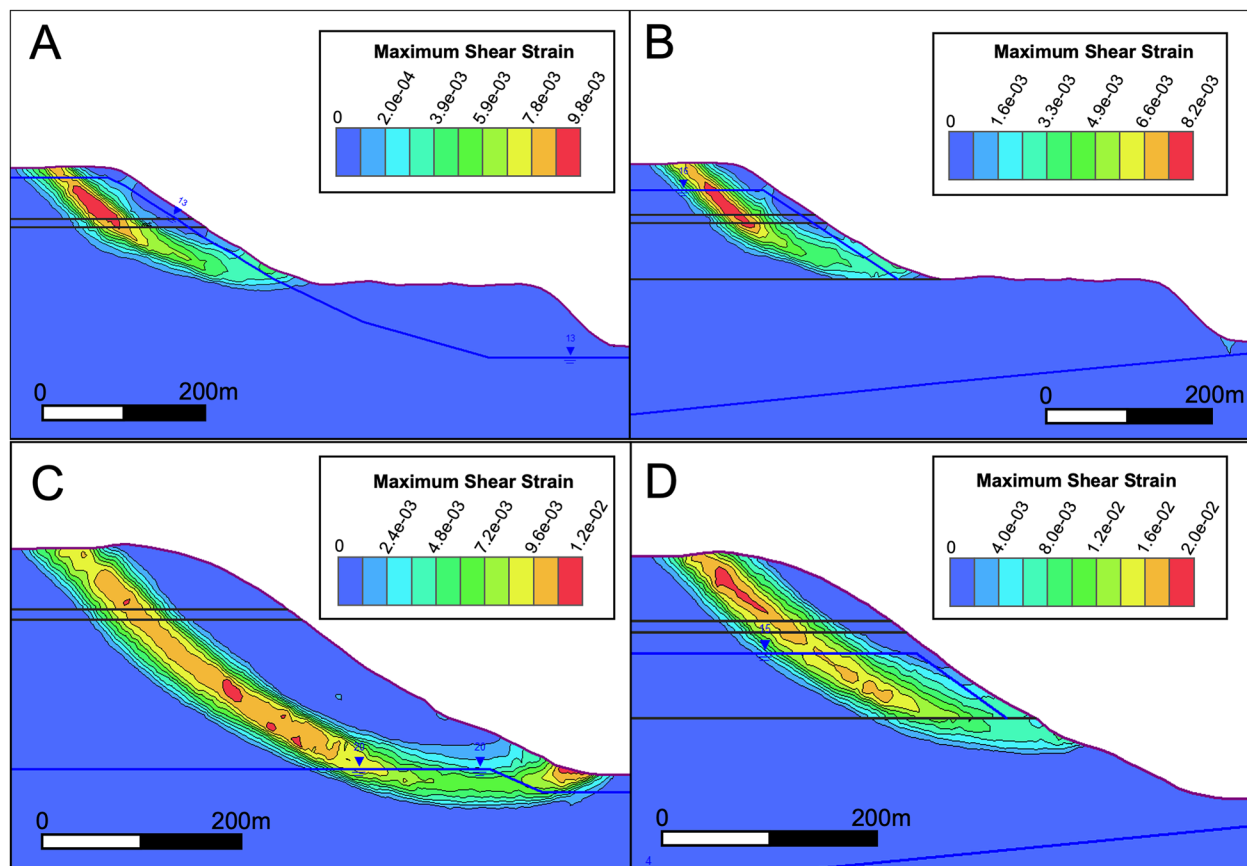


Fig. 10 RS2 modeling results showing the predicted shear surface (illustrated by maximum shear strain) at the landslide initiation depth for each slope and groundwater scenario. Dark blue lines represent water tables, while black lines represent model material boundaries. **A** Zarzal Landslide, single saturated zone; **B** Zarzal Landslide, two saturated zones; **C** Pachaqui Chico Landslide, single

saturated zone; **D** Pachaqui Chico Landslide, two saturated zones. In the case of Pachaqui Chico, the modeled perched water table produces a shallower shear surface than the single saturated zone. The Zarzal shear surface is similar for both groundwater scenarios, though a slight depth difference can be observed near the base of the perched zone

initiated by raising the original water table, assuming that the original water table sloped gently away from the Siguan River according to a typical losing stream groundwater profile (lower water table in Fig. 5D). The FEM models indicate that the water table would only need to be elevated to within 220–240 m of the top of the slope for landslide initiation to occur with a single saturated zone. However, this would also cause a deeper failure surface to form (Fig. 10C). No borings have been installed to check the failure depth at Pachaqui Chico; however, the model failure surface from Fig. 10C is likely too deep compared to the post-slide topography (compare Fig. 10C with Fig. 1(D) and Fig. 2B). In addition, the single groundwater system in 10C is too deep to account for the springs observed near Pachaqui Chico (Fig. 4A), even though it could initiate the landslide. Therefore, we conclude it is more likely that a perched zone formed at Pachaqui Chico as well.

As noted in the “Results” section, the Zarzal and Pachaqui Chico models have opposite responses to the different groundwater scenarios: the Zarzal models indicate a shallower landslide initiation depth with a single groundwater system, while the Pachaqui Chico models indicate a shallower landslide initiation

depth when two groundwater systems are present. We attribute the different responses to the different groundwater scenarios to changes in failure mode in the models. For Pachaqui Chico, the change in failure mode between groundwater scenarios is obvious (Fig. 10C, D), as the shear surface is noticeably shallower when a perched zone is included. For Zarzal, the difference in failure mode is more subtle (Fig. 10A, B) as a slight difference in the shear strain plot can be observed near the material boundary at the base of the perched zone Fig. 10B). When preparing models, the overall mesh density was held as consistent as possible, but using model material boundaries to control the perched zone inevitably results in some slight differences in the mesh, which can result in small changes to the model response.

In the analysis of increased unit weight of the unsaturated zone, while the overall model response is a decrease in FS with increasing unsaturated unit weight, many individual model cases did not fit well with this expected trend (Fig. 9). This variability is also likely related to the inherent precision level of FS values computed by the implementation of SSR in RS2. From multiple re-runs of identical models, we estimate this precision level to be around ± 0.03 in the value of FS. Based on this precision level, the increase in moisture

content does appear to affect model stability when the change in moisture content is high (17.5%). However, the scatter in the values suggests that the model design is not able to accurately resolve the difference in FS from smaller changes in moisture content. Five of the 16 moist unit weight models fall outside the estimated precision range of ± 0.03 compared to the base case value (Fig. 9). Of these, 4 cases are from Pachaqui Chico, in which changing the moisture content of the unsaturated zone affects a larger proportion of the material in the model (see Fig. 5C, D), implying that the effect of increased unit weight on slope stability may be greater for slopes in which the unsaturated zone(s) comprise a greater volume of the overall slope. As a result, we conclude that the influence of increased moist unit weight on slope stability is relatively small, given the input modeling conditions, and cannot be fully resolved by this modeling design. The implication of this is that the thickness and height of the saturated zone(s) is much more important to slope stability in this area than the additional weight resulting from saturation of previously unsaturated materials.

The results of this analysis provide additional evidence that perched zones are present in the NW slope of the Sigüas Valley. Considering that the probable depth of the natural groundwater system along the upper edge of the Sigüas Valley is at least ~ 250 m (from the crest of the slope to the level of the Sigüas River), it is more likely that the elevated groundwater levels necessary to initiate landsliding are achieved by perched groundwater systems, rather than the in situ system being elevated over 200 m. While perched groundwater systems can be laterally extensive in stratified rocks (Carter et al. 2011), it is not known how extensive or how consistent the depth of the perched zone is in this area. Local stratigraphy is flat-lying, but the presence of flow tuff units throughout the Paleogene-Neogene and Quaternary stratigraphy of the region (Jenks and Goldich 1956; Lebti et al. 2006) suggests the potential for hydrogeological heterogeneity in the subsurface, because flow tuffs can display significant lateral variability perpendicular to their flow paths. Laterally variable units could cause multiple small perched zones, which would also help to explain the variability in depth of the clay layer mapped by INRENA (2006) (Fig. 4A).

Comparison with other estimations of local groundwater conditions

Because the estimates of groundwater conditions at landslide initiation are based primarily on geomechanical modeling, it is useful to compare the modeling predictions with other more recent groundwater data. In 2019, measurement of piezometers NW and W-SW within 1 km of the Zarzal Landslide head scarp (Fig. 4A) showed water levels from 81 to 108 m below the ground surface (data collected 22 Jan 2019; Gonzales Zenteno E, 2021, personal communication). In addition, a resistivity profile was conducted in Summer 2019 about 2 km to the S-SW of the Zarzal Landslide (Flamme et al. 2020). This profile suggested a saturated zone (low resistivity) from about 100 to the max depth of the profile around 190 m below the top of the plateau. However, this profile reflects the groundwater about 2 km away from the Zarzal Landslide and was not deep enough to establish whether an unsaturated area exists below the indicated saturated zone (which would confirm the perched nature of the saturated zone).

Both sets of recent groundwater data collected are in good agreement with the critical groundwater level estimate for the Pachaqui Chico given a perched water table (90–100 m). However, at Zarzal, the recent data suggest that recent groundwater levels are deeper than the critical groundwater depths estimated in this analysis (10–40 m without a perched zone, 30–60 m depth with a perched zone). However, we tend to put more trust in shallower groundwater depths from this analysis because the Zarzal Landslide has clearly shown movement. The discrepancy between the recent data and the model-based estimates may possibly be accounted for by several possible causes: (1) The local water table at Zarzal was previously higher at the time of landslide initiation, and the landslide may have altered the local hydrogeology such that the piezometers near the headscarp now indicate a lower water table. About 14 years passed between the initiation of the Zarzal Landslide and the measurement of this more recent groundwater data. Also, average daily irrigation usage has decreased by a few m^3/s over the period of 2009–2017 (Wei X, personal communication, 2021), but this decrease is not likely to result in a lowering of the groundwater level of ~ 50 m. (2) The modeling effort presented in this paper has some inherent uncertainties (see also the “Results” and “Discussion of uncertainties related to model material properties” sections), which affect the precision of the critical groundwater depth estimates. (3) The subsurface heterogeneity is such that the depth of perched groundwater may vary by tens of meters over relatively small distance scales. This is supported by the variability in the depth of the interpreted clay layer mapped by INRENA (2006). The 2-km distance between the landslide and the resistivity profile is sufficient to capture some of this heterogeneity. (4) In addition, the industrial pond present to the NW of Zarzal (Fig. 4A) may have played a role in landslide initiation as well, which would help to account for the fact that the Zarzal Landslide occurred where it did, rather than on an adjacent section of slope.

In any case, the more recent groundwater data shows that water levels are elevated in the subsurface along the NW flank of the Sigüas Valley, and the modeling results show that elevated groundwater tables are required for landslide initiation for two slopes found along the valley flank. Because of the large change in groundwater depth that would be required to elevate the expected natural water table from below the base of the valley, even to a depth of 100 m below the top of the valley (about 150 m of change), it is more likely that perched groundwater is present and this is the main contributor to landslide initiation in the Sigüas Valley.

Discussion of uncertainties related to model material properties

The uncertainty in this analysis resulting from the use of back-calculated material property values (Graber et al. 2020) is worth acknowledging. Back-calculation of strength properties in slope stability analysis typically results in a non-unique solution, since several input parameters are often poorly constrained. Therefore, further analyses based on calibrated material properties inevitably retain the uncertainty from the calibration process. In addition, the material properties used for this analysis were calibrated using the Zarzal slope geometry, but were not calibrated to Pachaqui Chico (Graber et al. 2020). Because the two sites are about 9 km apart, it is possible that there is some variation between the two in strength properties or stratigraphy that has not been captured in

this analysis. However, because the overall stratigraphy is similar (INGEMMET 2008), and because the various rock types represented in the area seem to be fairly similar in their overall strength, we believe that the calibrated material property values are a reasonable approximation of the actual strength values.

The material strength parameters used in this analysis are relatively low for intact rock. However, given the geometry of these slopes, higher strength values corresponding to stronger intact rock would increase the FS values for both slopes. As a result, model failure would require an even higher groundwater table, or some other groundwater, stratigraphy, or strength condition that is currently unknown. As a result, even though the chosen material property values may seem low for large rock slopes, the fact is that the real slopes did fail given the geometries used in these models. The conclusion that these materials are relatively weak is also supported by widely observed raveling of roadcuts in conglomerate units of the Millo and Moquegua Fms., and by the history of landsliding in this valley, both since the start of irrigation and prior to irrigation.

Potential mitigation strategies

Because the Zarzal Landslide is currently moving, it has the potential to continue to present hazards to local residents. The Pachaqui Chico Landslide does not appear to be currently moving, but it represents a style of landslide that could occur again in the Sigüas Valley. In addition, recent groundwater data indicates that water levels along the NW valley flank are high enough (see the “[Comparison with other estimations of local groundwater conditions](#)” section) to potentially initiate new landslides in the style of Pachaqui Chico. So, landslide mitigation is likely to be beneficial for reducing future hazards and the likelihood of future failures. Because of the size of Zarzal and Pachaqui Chico, most mechanical mitigation methods are likely to be prohibitively expensive. Potentially useful mitigation methods include:

- Reducing irrigation input by using low water irrigation methods (drip) and by lining irrigation canals in order to reduce infiltration and lower the elevated groundwater table. This method has been shown to cause a reduction in landslide activity for other areas subject to irrigation-induced landslides (Clague and Evans 2003).
- Installation of pumping wells upstream of the NW valley flank to remove irrigation water from the subsurface and prevent that water from further elevating the water table or flowing into existing slide masses like Zarzal. If water is pumped, the discharge location should be chosen carefully, because discharge at the top of another slope along the Sigüas Valley or on a lower terrace could initiate a landslide there instead.
- Addition of passive drainage systems to existing slides, including drains installed within the slide mass itself, removing water from the area around the slide plane and funneling it to the downstream area. This can be useful for slopes that are actively deforming, though continual deformation can also quickly destroy drain structures.
- Implementation of setbacks: a “no-build” setback perimeter could be drawn along the upper edge of the NW Sigüas Valley flank. This perimeter could be used in land use planning to

prevent further development of roads, buildings, or agriculture within the expected area of influence of the landslide. The area above the Zarzal Landslide is particularly vulnerable, as the landslide threatens the Pan-American Highway, buildings, and an industrial facility. Though the threatened land elsewhere along the Sigüas Valley flank is primarily agricultural, more loss of land is likely if no mitigation is implemented.

Conclusion

We performed FEM modeling to estimate the critical groundwater conditions for the Zarzal and Pachaqui Chico Landslides, and found that, under our best estimate of the local geomechanical and hydrogeological conditions, elevated groundwater tables are necessary for landslide initiation at both slopes. Field measurements of groundwater levels provide evidence for elevated groundwater levels in the vicinity of both landslides. Observations of new springs, relatively low-permeability stratigraphy, the difference in elevation between the top of the slope and the probable in situ groundwater system, and the FEM stability analysis all imply that the elevated groundwater is perched. Compared to the height and configuration of the groundwater table, a changing moisture content of the unsaturated zone resulting from infiltration of irrigation water appears to be a relatively minor contributor to landslide initiation. Mitigation of elevated groundwater conditions is likely necessary for prevention of future landslides elsewhere along the Sigüas Valley, and these efforts should focus on reducing groundwater levels.

Acknowledgements

Funding for this project was provided by the Center for Mining Sustainability, a joint venture between the Universidad Nacional de San Agustín (Arequipa, Peru) and Colorado School of Mines (USA). Additional thanks go to colleagues at Colorado School of Mines: Hanna Flamme and Rich Krahenbuhl for advising on the results of the resistivity survey; and to Gabe Walton, for modeling advice. We would also like to thank Pascal Lacroix, ISTERre, University of Grenoble (France), for providing a 2 m DEM of the study area, and to the anonymous reviewers who provided helpful comments and feedback on the manuscript.

Author contribution

Conceptualization: AG, PS; methodology: AG, PS; formal analysis and investigation: AG; writing, first draft: AG; review and editing: AG, PS, PMA; approval of final draft: AG, PS, PMA; supervision: PS.

Funding

Center for Mining Sustainability.

Declarations

Conflict of interest The authors declare no competing interests.

References

Ali J, Nizami A, Hebinck P (2017) Mismanagement of irrigation water and landslides in Yourjogh. *Pakistan Mt Res Dev* 37(2):170–178. <https://doi.org/10.1659/MRD-JOURNAL-D-16-00045.1>

- Araujo G (2017) Área de Influencia del Deslizamiento de Sigwas y Geodinámico del Valle. Instituto Geológico Minero y Metalúrgico (INGEMMET), República del Perú, Informe Técnico No. A6772, 16p
- Araujo G, Taipei E, Miranda R, Valderrama P (2017) Dinámica y Monitoreo del Deslizamiento de Sigwas. Instituto Geológico Minero y Metalúrgico (INGEMMET), República del Perú. Informe Técnico No. A6748, 54p
- Araujo Huamán G, Miranda Cruz R (2016) Evaluación Geológica y Geodinámica de Deslizamientos en el Flanco Izquierdo del Valle de Vitor, Sectores Pie de Cuesta, Telaya, Gonzales y Socabón. Instituto Geológico Minero y Metalúrgico (INGEMMET), República del Perú, Informe Técnico No. A6722, 19p
- Araujo Huamán G, Valderrama Murillo P, Taipei Maquerhua E, Huarez Yarleque C, Díaz Apaza J, Miranda Cruz R (2016) Dinámica del Deslizamiento de Sigwas. Instituto Geológico Minero y Metalúrgico (INGEMMET), República del Perú. Informe Técnico No. A6715, 44p
- Beyabanaki SA, Bagtzoglou AC, Anagnostou EN (2016) Effects of groundwater table position, soil strength properties and rainfall on instability of earthquake-triggered landslides. *Environ Earth Sci* 75(4):1–13. <https://doi.org/10.1007/s12665-016-5277-2>
- Bradley K, Mallick R, Andikagumi H, Hubbard J, Meilianda E, Switzer A et al (2019) Earthquake-triggered 2018 Palu Valley landslides enabled by wet rice cultivation. *Nat Geosci* 12:935–939. <https://doi.org/10.1038/s41561-019-0444-1>
- Brönnimann CS (2011) Effect of groundwater on landslide triggering. Dissertation (No. 5236), École Polytechnique Fédérale de Lausanne, Switzerland
- Carter JTV, Gotkowitz MB, Anderson MP (2011) Field verification of stable perched groundwater in layered bedrock uplands. *Groundwater* 49(3):383–392. <https://doi.org/10.1111/j.1745-6584.2010.00736.x>
- Chiliza SG, Hingston EDC (2018) Back analysis of an ancient rockslide at lake Fundudzi, Limpopo Province. *South Africa Bull Eng Geol Environ* 77(1):29–47. <https://doi.org/10.1007/s10064-016-1001-4>
- Clague JJ, Evans SG (2003) Geologic framework of large historic landslides in Thompson River Valley. *British Columbia Environ Eng Geosci* 9(3):201–212. <https://doi.org/10.2113/9.3.201>
- domej G, aslanov U, ischuk A (2019) Geophysical investigations on the contribution of irrigation channels to landslide activity in Tuson. *Tajikistan J Himal Earth Sci* 52(2):161
- Fidel Smoll L, Valenzuela OG, Castro JS (1997) Estudio Geodinámico de la Cuenca de los Ríos Quilca, Sihuas Y Vitor, Departamento de Arequipa. Instituto Geológico Minero y Metalúrgico (INGEMMET), República del Perú. Serie C: Geodinámica y Ingeniería Geológica, Boletín No. 19. 250p
- Flamme HE, Sirota D, Krahenbuhl R, Li Y, Dugan B, Shragge J, Gonzales Zenteno E, Ticona Paucara, JR, Minaya Lizárraga (2020) Geophysical investigation to understand local geology and agricultural water movement in relation to landslide activity in Majes, Peru. SEG Technical Program Expanded Abstracts 2020. September 2020, 3341–3345
- García-Chevesich P, Wei X, Ticona J, Martínez G, Zea J, García V, Alejo F, Zhang Y, Flamme H, Graber A, Santi P et al (2021) The impact of agricultural irrigation on landslide triggering: a review from Chinese, English, and Spanish literature. *Water* 13(10). <https://doi.org/10.3390/w13010010>
- Gómez Avalos JC (2017) Evaluación geodinámica y modelamiento geotécnico del deslizamiento de madrigal – Arequipa. Universidad Nacional Mayor de San Marcos, Lima, Peru, Thesis
- Graber A, Santi P, Radach K, Meza Arestegui P, Chacon Arcaya S (2020) Finite element model calibration in the context of limited data and limited access: a case study from a large landslide in Southern Peru. *Proceedings of the 54th US Rock Mech/Geomech Symp*, Golden, CO, 28 June – 1 July 2020, Paper No. ARMA 20–1356
- Greco R, Marino P, Santonastaso GF, Damiano E (2018) Interaction between perched epikarst aquifer and unsaturated soil cover in the initiation of shallow landslides in pyroclastic soils. *Water* 10(7):948. <https://doi.org/10.3390/w10070948>
- Guizado Jol, J (1968) Geología del Cuadrángulo de Aplao. Servicio de Geología y Minería, República del Perú. Boletín, Serie A: Carta Geológica Nacional, No. 20. 57p
- Hammah RE, Yacoub TE, Corkum BC, Curran JH (2005) The shear strength reduction method for the generalized Hoek-Brown criterion. *Proceedings of the 40th US Symposium on Rock Mech.*, Anchorage, AK, 25–29 June 2005, Paper No. ARMA/USRMS 05–810
- Hermanns RL, Valderrama P, Fauqué L, Penna IM, Sepúlveda S, Moreiras S, Zalava Carrión B (2012) Landslides in the Andes and the need to communicate on an interandean level on landslides mapping and research. *Revista De La Asociación Geológica Argentina* 69(3):321–327
- Instituto Geológico Minero y Metalúrgico (INGEMMET) (2008) Mapa Geológico del Cuadrángulo Aplao, Hoja 33-r-1, Escala: 1:50,000, República del Perú
- Instituto Nacional de Recursos Naturales (INRENA) (2006) Estudio de Prospección Geofísica en un Sector de la Pampas de Majes (Flanco Derecho del Río Sigwas). Instituto Nacional de Recursos Naturales, Ministerio de Agricultura, República del Perú, 119p
- Jenks WF, Goldich SS (1956) Rhyolitic Tuff Flows in Southern Peru. *J Geol* 64(2):156–172. <https://doi.org/10.1086/626331>
- Knott JR (2008) The influence of irrigation on slope movements, Ventura County, California, USA. *Environ Eng Geosci* 14(3):151–165. <https://doi.org/10.2113/gsegeosci.14.3.151>
- Kosaka Masuno R, Minaya Lizárraga A, Arias Barahona HP, Ticona Paucara J, Farfán Bazán E, Campano Frisancho J (2001) Estudio Geodinámico y Evaluación de Peligros del Valle de Majes. Universidad Nacional de San Agustín de Arequipa, Proyecto PER 98/018 PNUD, 144p
- Lacroix P, Araujo GE, Hollingsworth J, Taipei E (2019) Self-entrainment motion of a slow-moving landslide inferred from Landsat-8 time series. *J Geophys Res: Earth Surf* 124:1201–1216. <https://doi.org/10.1029/2018JF004920>
- Lacroix P, Dehecq A, Taipei E (2020) Irrigation-triggered landslides in a Peruvian desert caused by modern intensive farming. *Nat Geosci* 13:56–60. <https://doi.org/10.1038/s41561-019-0500-x>
- Lebti P, Thouret JC, Wörner G, Fornari M (2006) Neogene and Quaternary ignimbrites in the area of Arequipa, Southern Peru: Stratigraphical and petrological correlations. *J Volc Geotherm Res* 154(3):251–275. <https://doi.org/10.1016/j.jvolgeores.2006.02.014>
- Li HJ, Jin YL (2012) Initiation analysis of an irrigation-induced loess landslide. *Appl Mech & Mater* 170–173:574–580. <https://doi.org/10.4028/www.scientific.net/AMM.170-173.574>
- Luque Poma G, Rosado Seminario M (2014) Zonas Críticas por Peligros Geológicos Región Arequipa. Instituto Geológico Minero y Metalúrgico (INGEMMET), República del Perú, Informe Técnico, 112p
- Manger E (1963) Porosity and Bulk Density of Sedimentary Rocks. *US Geological Survey Bulletin* 1144-E, 60p
- Meza Arestegui P, Chacon Arcaya S (2017) Evaluación Preliminar de las Condiciones Geodinámicas del Deslizamiento El Zarzal. Thesis, Universidad Nacional de San Agustín de Arequipa, Arequipa, Peru, Alto Sigwas
- Patton A, Rathburn S, Capps D (2019) Landslide response to climate change in permafrost regions. *Geomorphology* 340:116–128. <https://doi.org/10.1016/j.geomorph.2019.04.029>
- Peng J, Zhuang J, Wang G, Dai F, Zhang F, Huang W, Xu Q (2018) Liquefaction of loess landslides as a consequence of irrigation. *Quarterly J Eng Geol Hydrogeol* 51(3):330–337. <https://doi.org/10.1144/qjegh2017-098>
- Preisig G (2020) Forecasting the long-term activity of deep-seated landslides via groundwater flow and slope stability modelling. *Landslides* 17:1693–1702. <https://doi.org/10.1007/s10346-020-01427-1>
- Ray RL, Jacobs JM, de Alba P (2010) Impacts of Unsaturated Zone Soil Moisture and Groundwater Table on Slope Instability. *J Geotech and Geoenviron Eng* 136(10):1448–1458. [https://doi.org/10.1061/\(ASCE\)GT.1943-5606.0000357](https://doi.org/10.1061/(ASCE)GT.1943-5606.0000357)
- Roberti G, Ward B, van Wyk de Vries B, Araujo Huamán G, Aguilar Contreras R, Manrique Llerena N, Roberts NJ (2018) Estudio geomorfológico y paleoambiental de las avalanchas de escombros de Maca y Lari, Valle de Colca. *Proceedings of the Foro Internacional: Los Volcanes y Su Impacto*, Arequipa, Perú 2018:23–30
- Rocscience (2021) RS2 Theory Overview. Rocscience Inc. https://www.rocsience.com/help/rs2/theory/theory_overview.htm. Accessed 19 July 2021
- Salinas-Jasso JA, Montalvo-Arrieta JC, Chapa-Guerrero JR (2020) A dynamic stability analysis for the Olinalá landslide, northeastern Mexico. *Nat Hazards* 102:1225–1248. <https://doi.org/10.1007/s11069-020-03954-5>

- Smyth RC, Sharp Jr JM (2006) The hydrology of tuffs. In: Heiken G (ed) Tuffs—Their properties, uses, hydrology, and resources. Geol Soc Am Special Paper 408, pp 91–111. [https://doi.org/10.1130/2006.2408\(4.1\)](https://doi.org/10.1130/2006.2408(4.1))
- Van Asch ThWJ, Hendriks MR, Hessel R, Rappange FE (1996) Hydrological triggering conditions of landslides in varved clays in the French Alps. Eng Geol 42:239–251. [https://doi.org/10.1016/0013-7952\(95\)00082-8](https://doi.org/10.1016/0013-7952(95)00082-8)
- Van Asch ThWJ, Buma J, Van Beek LPH (1999) A view on some hydrological triggering systems in landslides. Geomorphology 30(1):25–32. [https://doi.org/10.1016/S0169-555X\(99\)00042-2](https://doi.org/10.1016/S0169-555X(99)00042-2)
- Villaseñor-Reyes CI, Dávila-Harris P, Hernández-Madrigal VM, Figueroa-Miranda S (2018) Deep-seated gravitational slope deformations triggered by extreme rainfall and agricultural practices (eastern Michoacan, Mexico). Landslides 15(9):1867–1879. <https://doi.org/10.1007/s10346-018-1031-z>
- Watkinson IM, Hall R (2019) Impact of communal irrigation on the 2018 Palu earthquake-triggered landslides. Nat Geosci 12:940–945. <https://doi.org/10.1038/s41561-019-0448-x>
- Wyllie DC, Mah CW (2004) Rock Slope Engineering: Civil and Mining, 4th edn. Spon Press, London and New York
- Xu L, Dai FC, Gong QM et al (2012) Irrigation-induced loess flow failure in Heifangtai Platform, North-West China. Environ Earth Sci 66:1707–1713. <https://doi.org/10.1007/s12665-011-0950-y>
- Zavala B, Nuñez JS, Gómez VD (2012) Estudio Geoambiental en la Cuenca Quilca-Vítor-Chili: Reporte Preliminar de Zonas Críticas por Peligros Geológicos. Instituto Geológico Minero y Metalúrgico (INGEMMET), República del Peru, Informe Técnico, 49p
- Zhang M, Liu J (2010) Controlling factors of loess landslides in western China. Environ Earth Sci 59(8):1671–1680. <https://doi.org/10.1007/s12665-009-0149-7>
- Zhang D, Wang G, Luo C, Chen J, Zhou Y (2009) A rapid loess flowslide triggered by irrigation in China. Landslides 6(1):55–60. <https://doi.org/10.1007/s10346-008-0135-2>
- Zhou Y, Qi S-C, Fan G, Chen M-L, Zhou J-W (2020) Topographic effects on three-dimensional slope stability for fluctuating water conditions using numerical analysis. Water 12(2):615. <https://doi.org/10.3390/w12020615>

Andrew Graber (✉) · **Paul Santi**

Department of Geology and Geological Engineering, Center for Mining Sustainability, Colorado School of Mines, 1500 Illinois St, Golden, CO 80401, USA
Email: apgrab@mines.edu psanti@mines.edu

Pablo Meza Arestegui

Facultad de Geología, Geofísica y Minas, Centro Para Minería Sostenible, Universidad Nacional de San Augustin de Arequipa, Santa Catalina Nro. 117, Arequipa, Peru
Email: pmezaa@unsa.edu.pe